Activation of Endoplasmic Reticulum Stress by Hyperglycemia Is Essential for Müller Cell–Derived Inflammatory Cytokine Production in Diabetes

Yimin Zhong,[1,2] Jingming Li,[1] Yanming Chen,[1,3] Joshua J. Wang,[1] Rajiv Ratan,[4] and Sarah X. Zhang[1,5]

Inflammation plays an important role in diabetes-induced retinal vascular leakage. The purpose of this study is to examine the role of endoplasmic reticulum (ER) stress and the signaling pathway of ER stress–induced activating transcription factor 4 (ATF4) in the regulation of Müller cell–derived inflammatory mediators in diabetic retinopathy. In diabetic animals, elevated ER stress markers, ATF4, and vascular endothelial growth factor (VEGF) expression were partially localized to Müller cells in the retina. In cultured Müller cells, high glucose induced a time-dependent increase of ER stress, ATF4 expression, and inflammatory factor production. Inducing ER stress or overexpressing ATF4 resulted in elevated intracellular adhesion molecule 1 and VEGF proteins in Müller cells. In contrast, alleviation of ER stress or blockade of ATF4 activity attenuated inflammatory gene expression induced by high glucose or hypoxia. Furthermore, we found that ATF4 regulated the c-Jun NH$_2$-terminal kinase pathway resulting in VEGF upregulation. ATF4 was also required for ER stress–induced and hypoxia-inducible factor-1α activation. Finally, we showed that administration of chemical chaperone 4-phenylbutyrate or genetic inhibition of ATF4 successfully attenuated retinal VEGF expression and reduced vascular leakage in mice with STZ-induced diabetes. Taken together, our data indicate that ER stress and ATF4 play a critical role in retinal inflammatory signaling and Müller cell–derived inflammatory cytokine production in diabetes. *Diabetes* 61:492–504, 2012

Diabetic retinopathy (DR) is a major complication of diabetes and often leads to severe visual disabilities. Recent studies reveal that chronic inflammation plays a causal role in the development and progression of DR. During diabetes, the retina expresses and produces high levels of proinflammatory cytokines, such as vascular endothelial growth factor (VEGF), and adhesion molecules, such as intercellular adhesion molecule (ICAM)-1, which are actively involved in various inflammatory responses in the diabetic retina. Depletion of ICAM-1 successfully abrogated retinal leukostasis, capillary cell death, and vascular leakage induced by diabetes

(1). Moreover, inhibition of VEGF by anti-VEGF therapies has demonstrated promising results in ameliorating diabetic macular edema in diabetic patients (2–4). Thus, identifying the key pathways that regulate inflammatory genes in retinal cells may elucidate new therapeutic targets for developing strategies to prevent retinal complications of diabetes.

Müller cells, the principal glial cells in the retina, are thought to be a major source of inflammatory factors in DR (5). These cells expand radially across almost the whole width of the retina, envelope neural synapses, and surround retinal capillaries. In addition, Müller cells express and secrete a number of growth factors and cytokines that alter the function and survival of retinal neurons and capillary cells. For example, Müller cells are activated at the early stage of DR (5), producing high levels of VEGF and expressing increased ICAM-1 when exposed to high glucose (HG) (6). Conditional deletion of VEGF in Müller cells significantly reduces leukostasis and vascular permeability in diabetic mice (7), suggesting that Müller cell–derived VEGF is important for retinal inflammation and vascular leakage in DR.

The endoplasmic reticulum (ER) is the primary cellular organelle responsible for protein maturation. Recent growing evidence suggests that the ER also acts as a principal stress sensor that through ER stress–triggered signaling pathways or unfolded protein response (UPR), regulates cell energy metabolism, redox status, inflammation, and cell survival (8–10). In a previous study, we showed that ER stress was increased in the retina of Akita mice, a spontaneous model of type 1 diabetes (11). Pharmaceutical induction of ER stress in nondiabetic mouse eyes increased retinal expression of inflammatory cytokine tumor necrosis factor (TNF)-α and VEGF. In contrast, inhibition of ER stress by chemical chaperone 4-phenylbutyrate (PBA) significantly reduced retinal VEGF levels in diabetic and ischemic retinas (11). These findings indicate that ER stress plays a causal role in retinal inflammation. However, the mechanisms underpinning ER stress–mediated inflammation are yet to be determined.

In the current study, we investigated how ER stress pathways regulate inflammatory genes in retinal Müller cells. Our results demonstrate that hyperglycemia- and hypoxia-induced ER stress stimulates activating transcription factor 4 (ATF4) activation, which cross talks with classic inflammatory signaling mediated by hypoxia-inducible factor (HIF)-1α and c-Jun NH$_2$-terminal kinase (JNK), leading to upregulation of inflammatory genes in retinal Müller cells. Inhibition of ATF4 or suppression of ER stress by chemical chaperones successfully reduces retinal inflammation and vascular permeability in diabetic animals, suggesting that anti–ER stress therapy may hold promise as a potential therapeutic for vascular leakage in DR.

RESEARCH DESIGN AND METHODS

Materials. Tunicamycin (TM) was obtained from Sigma-Aldrich (St. Louis, MO). PBA, tauroursodeoxycholic acid (TUDCA), and JNK inhibitor II (SP600125) were purchased from Calbiochem (San Diego, CA). Protease inhibitor cocktail, anti-VEGF, anti–ICAM-1, anti-ATF4, anti-CHOP (C/EBP homologous protein), antiphospho-JNK, and anti-JNK antibodies were purchased from Santa Cruz Biotechnology (Santa Cruz, CA). Anti-GS (glutamine synthase) antibody was obtained from Millipore (Billerica, MA). Antiphospho–eIF2-α (eukaryotic translation initiation factor 2-α) antibody was obtained from Cell Signaling Technology (Boston, MA). Anti–eIF2-α, anti-ERN1 (ER to nucleus signaling 1), and anti–HIF-1α antibodies were obtained from Novus Biologicals (Littleton, CO). Anti-KDEL (Lys-Asp-Glu-Leu), antiphospho–IRE1-α (inositol-requiring enzyme 1-α), and anti–β-actin antibodies were obtained from Abcam (Cambridge, MA). Horseradish peroxidase–conjugated or biotinylated secondary antibody, fluorescein isothiocyanate avidin, and DAPI were purchased from Vector Laboratories (Burlingame, CA). Cy3-conjugated anti-rabbit IgG was obtained from Jackson ImmunoResearch Laboratories (West Grove, PA).

Cell culture. Rat retinal Müller cells (rMC-1) were supplied by Vijay Sarthy (Northwestern University, Evanston, IL) and maintained in Dulbecco's modified Eagle's medium (DMEM) containing 10% FBS and 1% antibiotic/antimycotic solution. To determine the expression of phospho–eIF2-α, phospho–IRE1-α, and glucose regulated protein 78 (GRP78) in response to HG, 80% confluent rMC-1 were quiescent in DMEM with 1% FBS for 8 h followed by treatment with HG (25 mmol/L), normal glucose (5 mmol/L), or mannitol (25 mmol/L) for 0–24 h. To detect the expression of ATF4, CHOP, ICAM-1, and VEGF in response to HG, 50% confluent rMC-1 were treated in DMEM supplemented with 0.5% BSA containing HG, normal glucose, or mannitol with daily medium replacement for 72 h. Cells were harvested for biochemical or immunocytochemical assays.

Animal studies. C57BL/6 J mice were purchased from The Jackson Laboratory (Bar Harbor, ME). Care, use, and treatment of all animals were in strict agreement with the guidelines of the Association for Research in Vision and Ophthalmology Statement for the Use of Animals in Ophthalmic and Visual Research and approved by the institutional animal care and use committees in the University of Oklahoma Health Sciences Center. To induce diabetes, 8-week-old C57 mice were given five consecutive intraperitoneal injections of streptozotocin (STZ; 50 mg/kg body wt/day) (Sigma-Aldrich) or vehicle as control. Four weeks after STZ injection, mice were humanely killed and eyes harvested for analyses.

Periocular and intravitreal injection. Periocular injection was used for repeated delivery of PBA into the retina in diabetic mice as described previously (11). Intravitreal injection was used for single delivery of adenovirus into the vitreous using an UltraMicroPump (World Precision Instruments, Sarasota, FL) (12). In brief, under a dissection microscope, an incision was made 1 mm behind the limbus with a sharp-edge 31-gauge needle in deeply anesthetized mice. The 34-gauge blunt needle mounted on a 10-μL microsyringe was inserted into the vitreous cavity. One microliter of vehicle containing 10^9 viral particles was delivered into the vitreous with one depression of the foot switch.

Adenovirus infection of rMC-1 cells. Adenoviruses expressing wild-type ATF4 (Ad-ATF4WT) or a dominant negative mutant of ATF4 (Ad-ATF4DN) were generated as described previously (13). Adenovirus-expressing green fluorescent protein (Ad-GFP) was used as a control. rMC-1 cells were infected with adenoviruses at a multiplicity of infection of 10 or 20. Twenty hours after infection, the adenovirus was removed and cells were cultured in DMEM containing 0.5% BSA and 5 mmol/L glucose for 24 h to acquire quiescent before desired treatment.

Immunocytochemistry. Cells were fixed with ice-cold acetone for 10 min. After blocking with 3% BSA in phosphate-buffered saline for 1 h, cells were incubated with rabbit anti–HIF-1α antibody (1:400) overnight at 4°C followed by secondary Cy3-conjugated affinity-purified donkey anti-rabbit IgG (1:400) at room temperature for 1 h. Nuclei were stained with DAPI. Slides were visualized and photographed under a fluorescent microscope (Olympus AX70; Olympus America, Center Valley, PA).

Immunohistochemistry. For frozen sections, the cornea and lens were removed and the eyecups were fixed with 4% paraformaldehyde for 30 min. Eyecups were then cryoprotected with a series of sucrose solution (10–30%) and cross sections of the retina were obtained using a cryostat. Retinal sections were immunostained using anti-GS (1:600), antiphospho–eIF2-α (1:100), anti-ATF4 (1:150), anti-GADD153 (1:100), and anti-VEGF (1:100) antibodies overnight at 4°C, followed by Cy3-conjugated or biotinylated secondary antibody and fluorescein isothiocyanate avidin. The fluorescence was visualized under an Olympus AX70 microscope.

Western blot analysis. Cells and retinas were lysed in radioimmunoprecipitation assay lysis buffer. Western blot analysis was performed as described previously (14). Primary antibodies used include antiphospho–eIF2-α (1:1,000), anti–eIF2-α (1:5,000), anti-KDEL (1:5,000), anti–IRE1-α (1:1,000), anti-ERN1, anti–ICAM-1 (1:500), anti-VEGF (1:500), anti–HIF-1α (1:2,000), anti-ATF4 (1:500), anti-GADD153 (1:500), antiphospho-JNK (1:500), anti-JNK (1:500), and anti–β-actin (1:5,000) antibodies.

Statistical analysis. Values are expressed as mean $\pm$ SD. Statistical analyses were performed using one-way ANOVA with Bonferroni multiple comparison test when comparing three or more groups or Student t test when comparing two groups. Statistical differences were considered significant at $P < 0.05$.

RESULTS

Activation of ER stress and ATF4 in retinal Müller cells in STZ-induced diabetic mice. STZ-induced diabetes in mice is a commonly used model to study nonproliferative DR. We examined retinal expression and cellular localization of ER stress markers in this model at 4 weeks after STZ injection. The markers include phosphorylated ER membrane proteins, RNA-dependent protein kinase–like ER kinase (PERK), and IRE1-α and the downstream effectors of the PERK pathway, including phosphorylated eIF2-α (p–eIF2-α), ATF4, and CHOP. We found that in the diabetic retina, p–eIF2-α level was markedly increased and partially colocalized with Müller cell marker GS (Fig. 1A and B). In addition, expression of ATF4 and its major target gene CHOP were drastically increased (Fig. 1A and B). In contrast to the cytosolic distribution of p–eIF2-α, intensive signals of ATF4 and CHOP, both of which are transcription factors, were observed in the nuclei of cells in the ganglion cell layer (GCL) and inner nuclear layer (Fig. 1A). Phosphorylation of IRE1-α was also significantly increased (Fig. 1B). Moreover, VEGF, a potent proinflammatory and propermeability factor, was significantly upregulated in the diabetic retina and colocalized with ATF4 expression (Fig. 1B and C).

HG induces ER stress and upregulation of ATF4 in rMC-1 cells. We next determined if hyperglycemia is sufficient to induce ER stress and ATF4 activation in retinal Müller cells. Rat rMC-1 cells were exposed to HG (25 mmol/L), normal glucose (5 mmol/L), or mannitol (25 mmol/L) for 0–72 h. ER stress markers including GRP78, phosphorylation of IRE1-α and eIF2-α, and expression of ATF4 and CHOP were measured by Western blot analysis. The results show that HG treatment induced a rapid upregulation of GRP78 (Fig. 2A and B), accompanied by increased phosphorylation of IRE1-α (Fig. 2A and C) and eIF2-α (Fig. 2A and D). ATF4 and CHOP expression was significantly increased 72 h after HG treatment, suggesting a time-dependent induction of ER stress and the UPR pathway by HG (Fig. 2E and F). Furthermore, coincubation of cells with chemical chaperone PBA dose dependently attenuated ATF4 and CHOP expression in HG-treated cells. This indicates that HG-induced ATF4 upregulation is secondary to ER stress.

ER stress stimulates ICAM-1 and VEGF production and mediates HG-induced inflammatory gene expression in rMC-1 cells. To address the effect of ER stress on inflammatory gene expression, rMC-1 cells were exposed to TM, a classic ER stress inducer, for 24 h. Expression of ICAM-1 and VEGF was measured by Western blot analysis. The results show that ER stress significantly increased protein levels of ICAM-1 by almost 2-fold (Fig. 3A and B) and VEGF by 2.5-fold (Fig. 3A and C) in Müller cells. Next, we determined if ER stress plays a role in HG-induced inflammatory gene expression. We found that HG treatment, but not mannitol, significantly increased ICAM-1 and VEGF expression in rMC-1 cells (Fig. 3D and E). Both PBA and TUDCA dose dependently reduced HG-induced ICAM-1 and VEGF expression (Fig. 3D and E). These results indicate that ER stress is implicated in HG-induced inflammatory gene expression in Müller cells.

ATF4 regulates ICAM-1 and VEGF expression in rMC-1 cells. Previous studies show that ATF4 is required for proinflammatory gene expression in vascular cells (15,16).
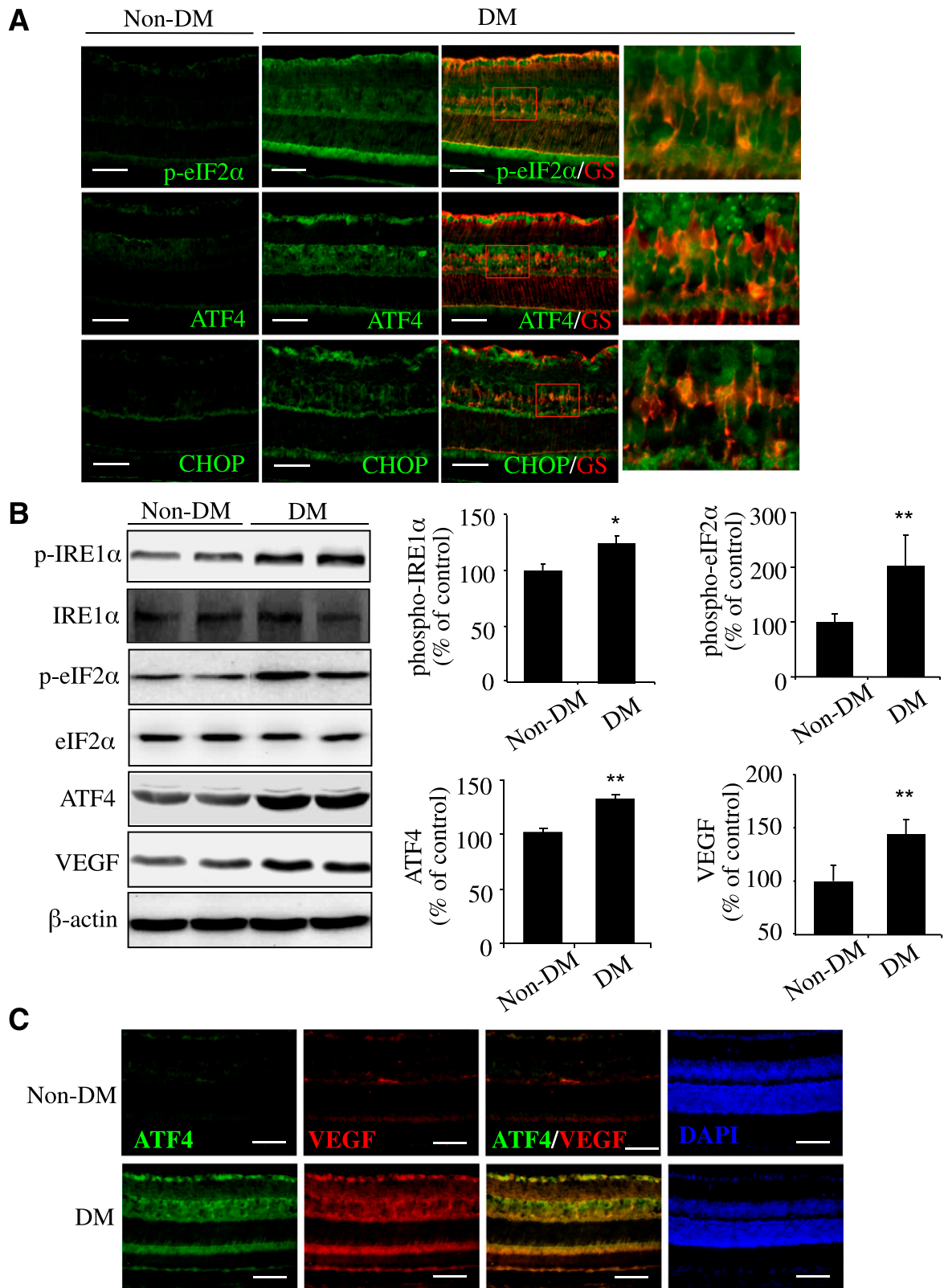
FIG. 1. Activation of ER stress and upregulation of ATF4 colocalized with VEGF in retinal Müller cells in diabetic mice. Diabetes (DM) was induced in 8-week-old C57 mice by five consecutive STZ injections (50 mg/kg/day). ER stress markers in the retina were examined at 4 weeks after STZ injection. *A*: Immunohistochemistry showing increased p–eIF2-α/ATF4/CHOP (green) partially colocalized with Müller cell marker GS (red) in diabetic retinas. Scale bar = 50 μm. *B*: Western blot analysis showing increased phosphorylation of IRE1-α and eIF2-α and elevated ATF4 and VEGF expression in diabetic retina. Bar graphs represent quantification results using densitometry (mean ± SD, *n* = 4). *$P < 0.05$, **$P < 0.01$ vs. control. *C*: Double staining of ATF4 (green) and VEGF (red) in retinal sections from diabetic and control mice. Scale bar = 50 μm. (A high-quality digital representation of this figure is available in the online issue.)
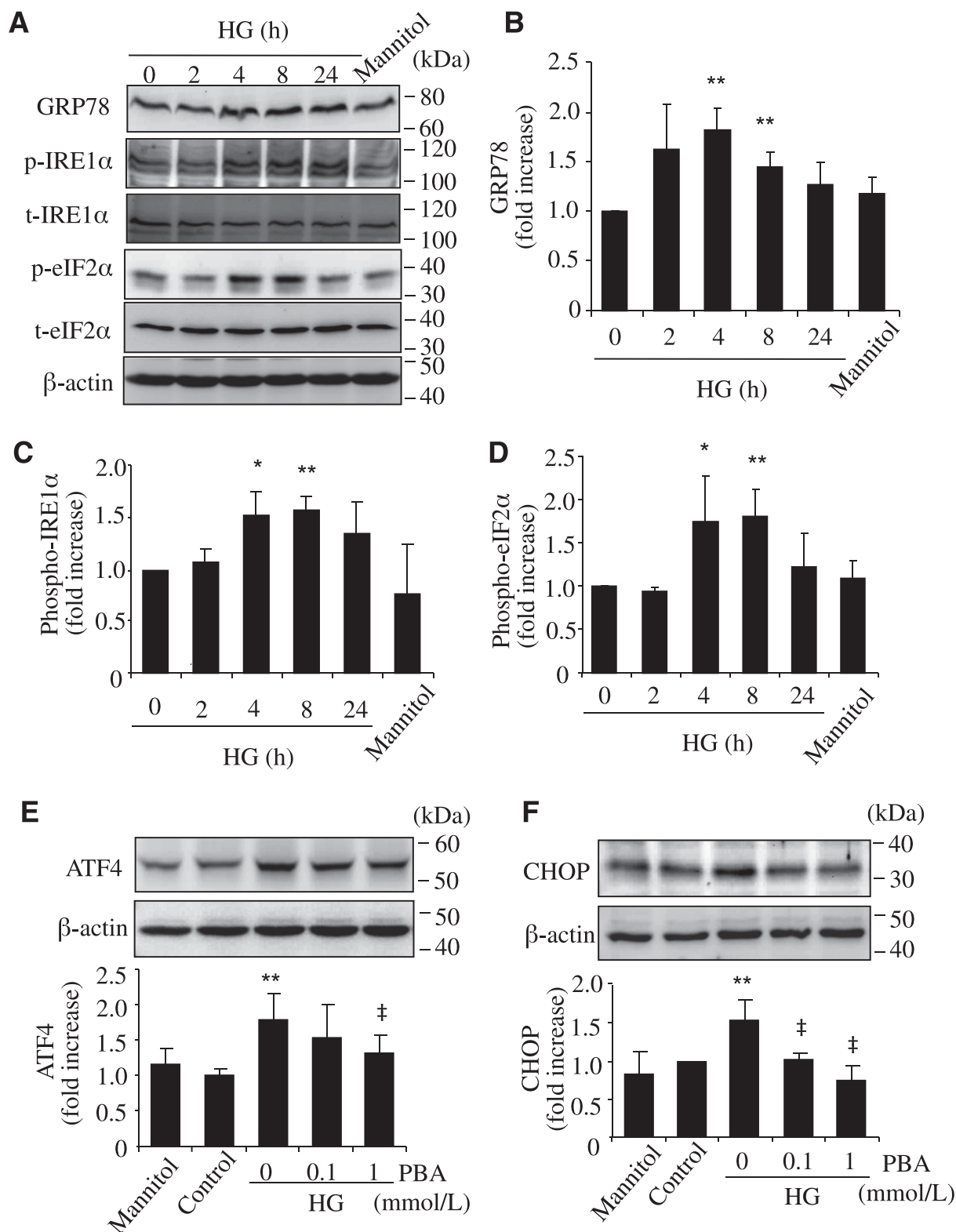
FIG. 2. Increased expression of ER stress markers by HG in rMC-1 cells. rMC-1 cells were treated with HG (25 mmol/L) or same concentration of mannitol for 2, 4, 8, or 24 h. ER stress markers were determined by Western blot analysis. *A*: Representative blots from three independent experiments. Expression of GRP78 (*B*), p–IRE1-α (*C*), and p–eIF2-α (*D*) were quantified by densitometry (mean ± SD, $n = 3$). *$P < 0.05$, **$P < 0.01$ vs. control. *E* and *F*: rMC-1 cells were treated with HG with or without chemical chaperone PBA for 72 h. Expression of ATF4 (*E*) and CHOP (*F*) were determined by Western blot analysis and quantified by densitometry (mean ± SD, $n = 3$). **$P < 0.01$ vs. control. ‡$P < 0.05$ vs. HG.
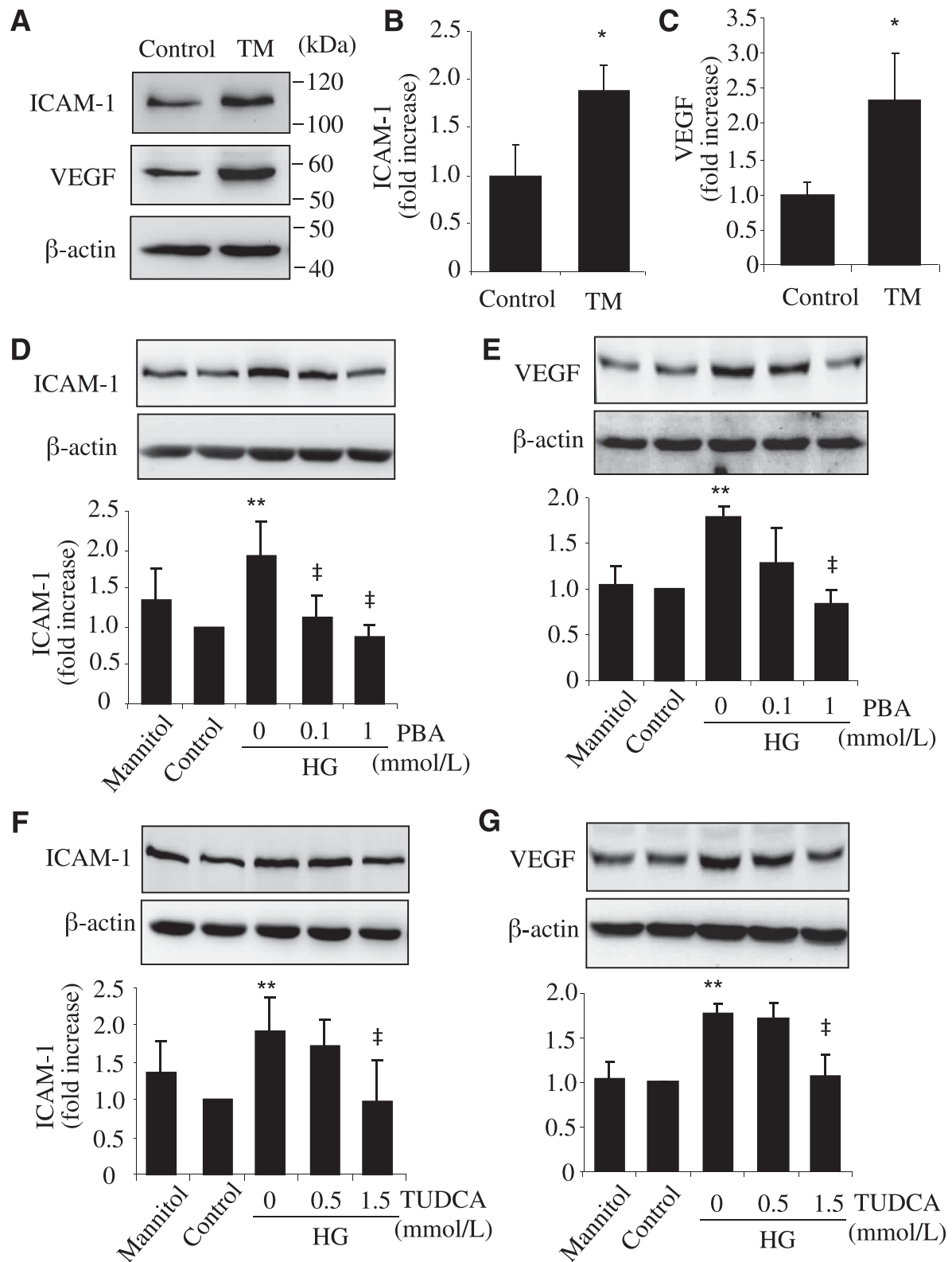
FIG. 3. ER stress is implicated in HG-induced ICAM-1 and VEGF expression in rMC-1 cells. *A–C*: rMC-1 cells were treated with 0.5 μg/mL TM for 24 h. Expression of ICAM-1 and VEGF were determined with Western blot analysis and quantified by densitometry (mean ± SD, *n* = 3). **P* < 0.05 vs. control. *D–G*: rMC-1 cells were treated with HG with or without chemical chaperone PBA (*D* and *E*) or TUDCA (*F* and *G*) for 72 h. Expression of ICAM-1 (*D* and *F*) and VEGF (*E* and *G*) were determined by Western blot analysis (mean ± SD, *n* = 3). ***P* < 0.01 vs. control. ‡*P* < 0.05 vs. HG.

To assess the potential role of ATF4 in Müller cells, we manipulated ATF4 expression and/or activity using Ad-ATF4WT or Ad-ATF4DN (13) in rMC-1 cells. Twenty-four hours after adenoviral treatment, cells were incubated with HG for 72 h or exposed to hypoxia conditions for 16 h. We found that overexpressing Ad-ATF4WT resulted in a significant increase in ICAM-1 and VEGF levels (Fig. 4*A*). Inhibiting ATF4 activity by Ad-ATF4DN had no effect on
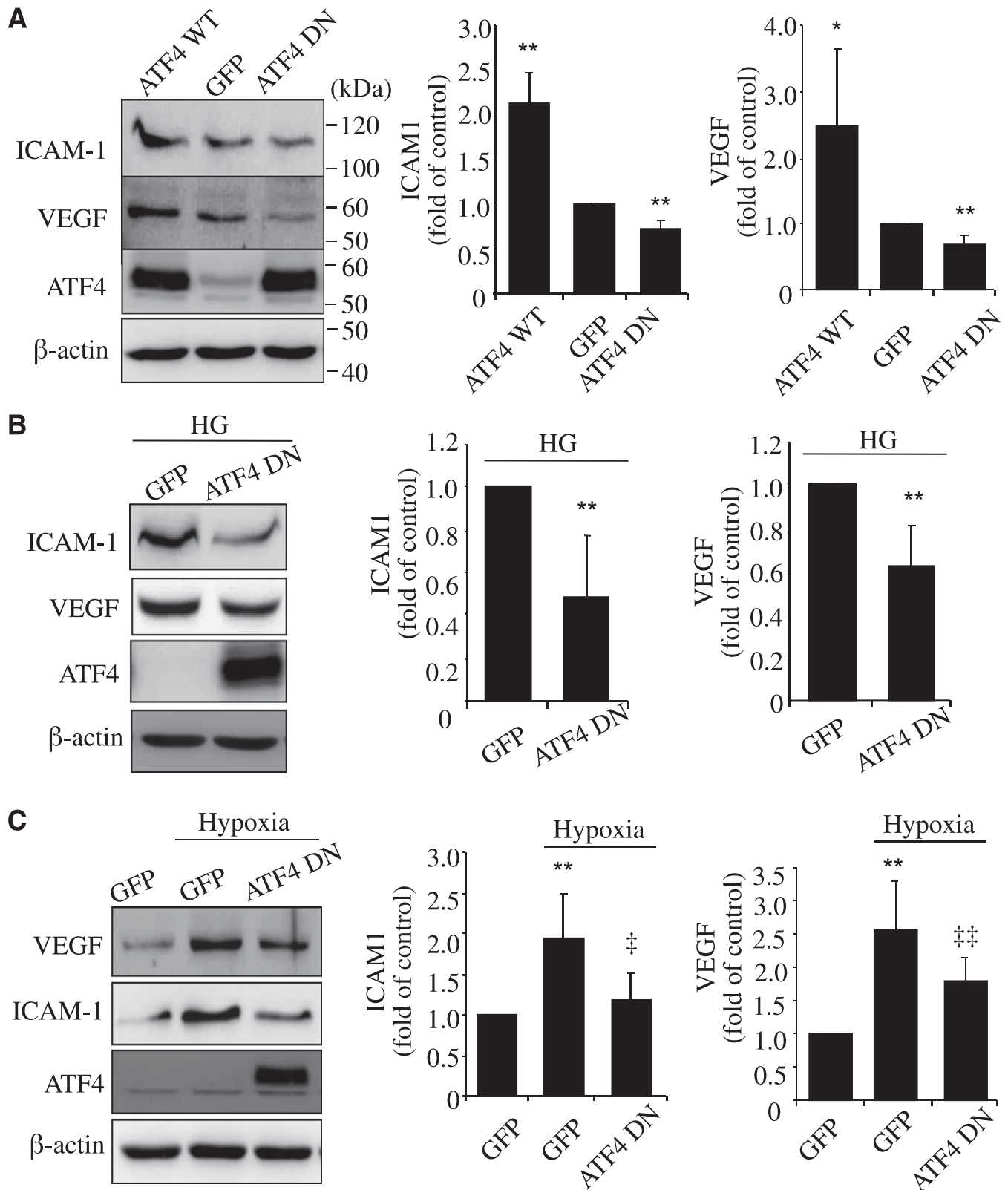
FIG. 4. ATF4 mediates HG- and hypoxia-induced ICAM-1 and VEGF upregulation in rMC-1 cells. *A*: rMC-1 cells were transfected with Ad-GFP, Ad-ATF4WT, or Ad-ATF4DN for 24 h. Expression of ICAM-1 and VEGF was determined by Western blot analysis and quantified by densitometry. *B* and *C*: rMC-1 cells were infected with Ad-GFP or Ad-ATF4DN for 24 h. After infection, cells were incubated with HG medium for 72 h (*B*) or exposed to hypoxia for 16 h (*C*). Expression of ICAM-1 and VEGF was measured by Western blot analysis and quantified by densitometry. Results are expressed as mean ± SD (*n* = 3). *$P < 0.05$, **$P < 0.01$ vs. Ad-GFP. ‡$P < 0.05$, ‡‡$P < 0.01$ vs. Ad-GFP plus hypoxia.
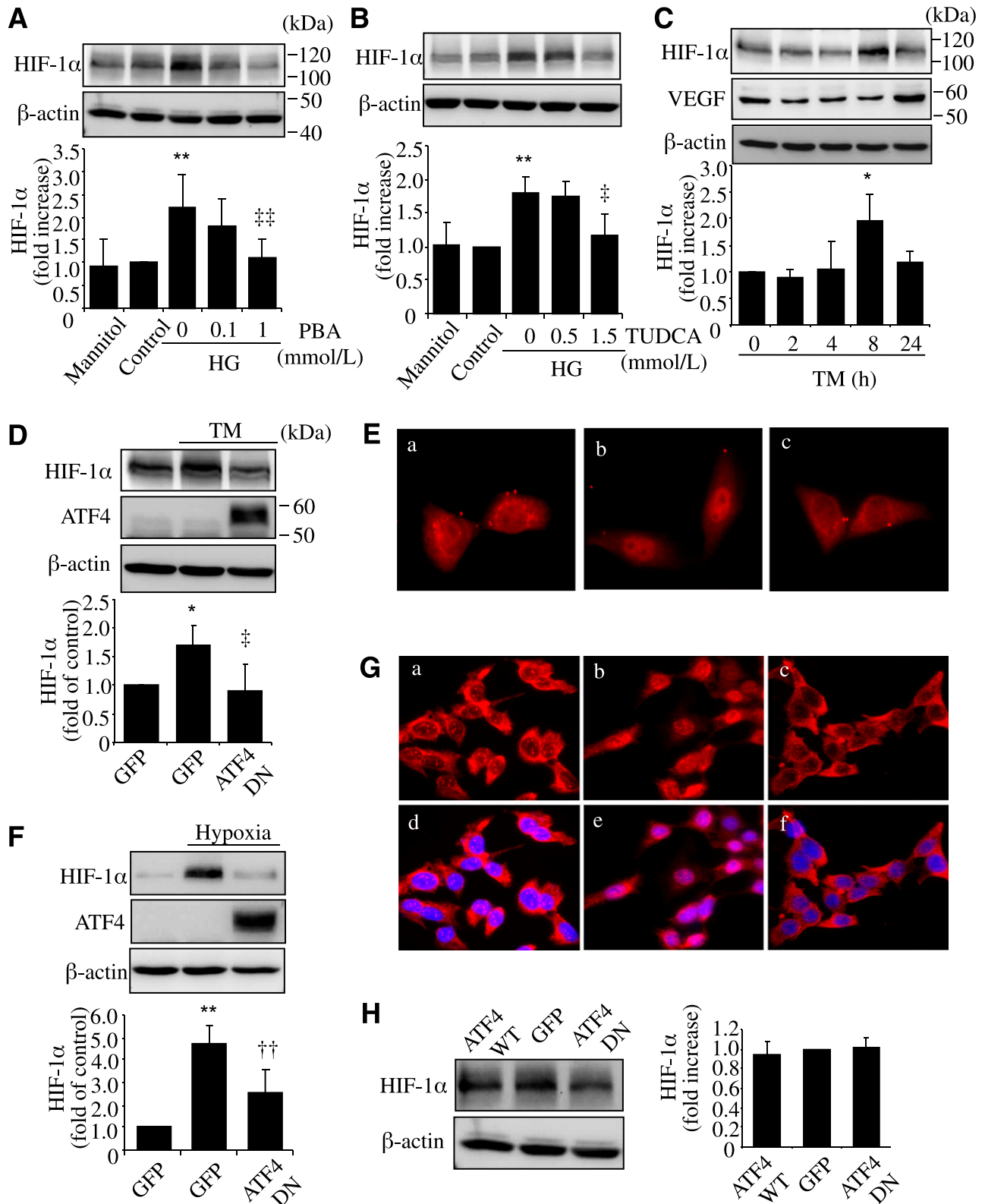
FIG. 5. ER stress and ATF4 are required for HG- or hypoxia-induced HIF-1α accumulation in rMC-1 cells. *A* and *B*: rMC-1 cells were treated with HG with or without chemical chaperone PBA or TUDCA for 72 h. Mannitol was used for osmotic control. Protein level of HIF-1α was measured by Western blot analysis and quantified by densitometry. **$P < 0.01$ vs. control. ‡$P < 0.05$, ‡‡$P < 0.01$ vs. HG. *C*: rMC-1 cells were treated with 0.5 μg/mL TM for 2, 4, 8, or 24 h. Protein level of HIF-1α and VEGF was determined by Western blot analysis and quantified by densitometry. *$P < 0.05$ vs. control. *D* and *E*: rMC-1 cells were transfected with Ad-ATF4DN or Ad-GFP for 24 h followed by treatment with 0.5 μg/mL TM for 8 h. Expression of HIF-1α (*D*) was determined by Western blot analysis and quantified by densitometry. *$P < 0.05$ vs. GFP, ‡$P < 0.05$ vs. GFP+TM. Cellular distribution of HIF-1α (*E*) was examined by immunocytochemistry. a, Ad-GFP; b, Ad-GFP+TM; c, Ad-ATF4DN+TM. *F* and *G*: After infection with Ad-ATF4DN or Ad-GFP, rMC-1 cells were exposed to hypoxia for 2 h. Expression of HIF-1α (*F*) was determined by Western blot analysis and quantified by densitometry. **$P < 0.01$ vs. GFP, ††$P < 0.01$ vs. GFP+hypoxia. Immunostaining of HIF-1α (*G*) showing hypoxia-induced nuclear translocation of HIF-1α in Ad-GFP–treated cells but not in Ad-ATF4DN–treated cells. a–c, HIF-1α staining; d–f, merged images of HIF-1α

the basal level of ICAM-1 but decreased VEGF expression in unstimulated cells (Fig. 4A). Moreover, blockade of ATF4 activity remarkably reduced ICAM-1 and VEGF in cells exposed to HG (Fig. 4B). It also significantly attenuated hypoxia-induced ICAM-1 and VEGF expression (Fig. 4C). These data indicate that ATF4 is a key regulator of VEGF and ICAM-1 expression in retinal Müller cells.

ER stress upregulates HIF-1α expression and nuclear translocation through ATF4 in rMC-1 cells. HIF-1α is a critical transcription factor that induces VEGF during hypoxia and diabetes (17). We evaluated the potential role of ER stress in the regulation of HIF-1α in Müller cells. We found that HG treatment for 72 h induced a marked increase in HIF-1α level in rMC-1 cells, which was effectively attenuated by PBA and TUDCA (Fig. 5A and B). Moreover, treatment of cells with TM led to a significant increase in HIF-1α level, followed by an increase of VEGF expression (Fig. 5C). This suggests that ER stress contributes to HG-induced HIF-1α increase in Müller cells. Next, we examined if ATF4 plays a role in ER stress–mediated HIF-1α regulation. We found that inhibiting ATF4 activity by Ad-ATF4DN completely abolished TM-induced HIF-1α increase in rMC-1 cells (Fig. 5D). Moreover, ATF4 inhibition also blocked the translocation of HIF-1α from cytoplasm to nucleus induced by TM (Fig. 5E). In a similar manner, suppressing ATF4 activity prevented hypoxia-induced HIF-1α upregulation (Fig. 5F) and nuclear translocation (Fig. 5G) in rMC-1 cells. It is intriguing that overexpressing Ad-ATF4WT or Ad-ATF4DN did not affect the basal level of HIF-1α (Fig. 5H), suggesting that ATF4 may be implicated in the regulation of HIF-1α only in conditions with enhanced ER stress.

Activation of JNK by ER stress and ATF4 mediates HG-induced VEGF expression in rMC-1 cells. Recent studies suggest that JNK is a key molecule that links ER stress to inflammation in intestinal epithelial cells (18). Activation of JNK is also required for VEGF expression in retinal cells (19). We examined if the JNK pathway is implicated in HG-induced inflammation in rMC-1 cells. Our results demonstrate that activation of JNK1 was significantly upregulated in cells after exposure to HG for 72 h, which was dose dependently inhibited by PBA and TUDCA (Fig. 6A and B). In addition, phosphorylated JNK1 was markedly increased by ER stress in rMC-1 cells (Fig. 6C). These results suggest that activation of JNK by HG, at least partially, is through ER stress. To further examine if activation of JNK plays a role in ER stress–mediated VEGF expression, we pretreated rMC-1 cells with SP600125, a selective JNK inhibitor, and then exposed cells to TM or infected cells with Ad-ATF4WT. We found both TM and Ad-ATF4WT induced a significant increase in JNK1 activation, accompanied by elevated VEGF expression (Fig. 6D and E). Inhibiting JNK activity by SP600125 remarkably attenuated VEGF expression in a dose-dependent manner (Fig. 6D and E). This suggests that JNK activation is required for ER stress– and ATF4-induced VEGF expression. Furthermore, we found that inhibition of ATF4 largely abolished JNK activation in rMC-1 cells induced by HG, indicating an essential role of ATF4 in HG-triggered JNK activation (Fig. 6F). These results collectively indicate that activation of JNK by ER stress and ATF4 contributes to HG-induced VEGF upregulation in retinal Müller cells.

Inhibition of ER stress or ATF4 alleviates retinal inflammatory gene expression and mitigated retinal vascular leakage in STZ-induced diabetic mice. We previously showed that induction of ER stress by TM increases inflammatory gene expression in normal mouse retinas (11). Here we determined if overexpression of ATF4 is sufficient to induce inflammatory genes in vivo. Adult C57BL/6 mice were given intravitreal injection of Ad-GFP or Ad-ATFWT (1×10^9 viral particles per eye). Two weeks later, mice were killed and retinas collected for analysis. We found that overexpressing Ad-ATF4WT induced a 2.4-fold increase in retinal TNF-α expression and a nearly 3-fold increase in ICAM-1 expression, when compared with Ad-GFP–treated eyes, suggesting ATF4 is a potent inducer of inflammatory genes in the retina (Fig. 7A). Next, we evaluated the effects of inhibition of ATF4 on retinal inflammation in STZ-induced diabetic mice. ATF4 activity was suppressed by intravitreal injection of Ad-ATF4DN in STZ-induced diabetic mice immediately after the onset of hyperglycemia. Three weeks after injection, retinal ICAM-1 and TNF-α levels were significantly reduced in eyes receiving Ad-ATF4DN treatment when compared with Ad-GFP–treated eyes (Fig. 7B). These results indicate a crucial role of ATF4 in diabetes-induced inflammatory gene expression in the retina.

Finally, we evaluated the therapeutic effects of pharmacological ER stress inhibitor on retinal inflammation and vascular leakage in STZ-induced diabetic mice. After the onset of diabetes, the mice received periocular injections of PBA (0.4 µmol/eye) into one eye and the same amount of vehicle into the contralateral eye twice a week for 6 weeks. Retinal level of VEGF was determined by Western blot analysis, and vascular permeability was measured by the Evans blue albumin method (20,21). Results show that periocular injection of PBA significantly decreased retinal VEGF level in STZ-induced diabetic mice (Fig. 7C). Moreover, vascular permeability was significantly increased in the diabetic retina, which was almost completed abolished in PBA-treated eyes when compared with vehicle-treated eyes (Fig. 7C and D). Furthermore, we did an immunofluorescence study of VEGF in the retina from mice after PBA or Ad-ATF4DN treatment. We found that both PBA and Ad-ATF4DN treatment effectively reduced VEGF expression in the retina, and in Müller cells, indicated by coimmunolabeling with GS, a Müller cell marker (Fig. 7E and F). These results corroborate our previous findings in Akita mice (11), strongly suggesting a causal role of ER stress and ATF4 in inflammatory gene expression and vascular leakage in DR. Taken together, our data indicate that activation of ER stress by hyperglycemia and hypoxia triggers ATF4 activation in retinal Müller cells. This in turn upregulates inflammatory gene expression, through directly binding to the promoters of genes or indirectly activating other inflammatory pathways such as JNK and HIF-1α, leading to retinal inflammation and vascular leakage (Fig. 8).

DISCUSSION

Compelling evidence suggests a role for ER stress in chronic inflammatory diseases, such as inflammatory bowel diseases, diabetes, and atherosclerosis (22–24). We previously

---

(red) and nuclear staining with DAPI (blue). a and d, Ad-GFP; b and c, Ad-GFP plus hypoxia; c and f, Ad-ATF4DN plus hypoxia. *H*: rMC-1 cells were infected with Ad-ATF4WT, Ad-ATF4DN, or Ad-GFP for 24 h. Expression of HIF-1α was determined by Western blot analysis and quantified by densitometry (mean ± SD, $n = 3$). (A high-quality digital representation of this figure is available in the online issue.)
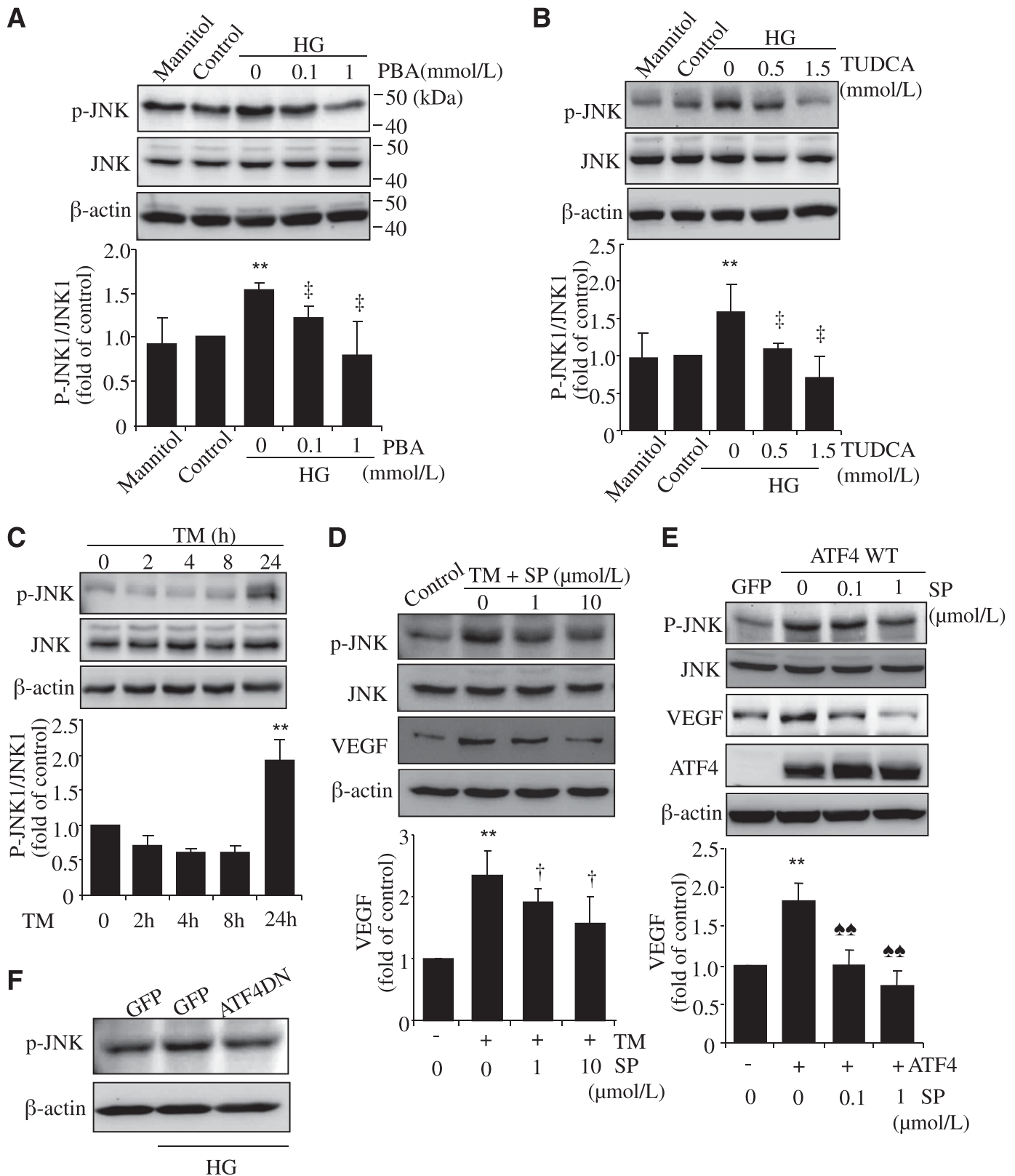
FIG. 6. Activation of JNK by ER stress and ATF4 contributes to HG-induced VEGF expression in rMC-1 cells. rMC-1 cells were treated with HG with or without chemical chaperone PBA (*A*) or TUDCA (*B*) for 72 h. Mannitol was used for osmotic control. *C*: rMC-1 cells were treated with 0.5 μg/mL TM for 2, 4, 8, or 24 h. Phosphorylation of JNK1 was determined by Western blot analysis and quantified by densitometry. *D*: rMC-1 cells were preincubated with 1 or 10 μmol/L SP600125 (SP) for 1 h, followed by treatment with 0.5 μg/mL TM for 24 h. *E*: rMC-1 cells were preincubated with 0.1 or 1 μmol/L SP for 1 h, followed by transfection with Ad-ATF4WT for 24 h. Expression of VEGF and JNK was determined by Western blot analysis. Protein level of VEGF was quantified by densitometry. Values are expressed as mean ± SD (*n* = 3). **$P < 0.01$ vs. control; ‡$P < 0.05$ vs. HG; †$P < 0.05$ vs. TM; ♠♠$P < 0.01$ vs. Ad-ATF4. *F*: rMC-1 cells were transfected with Ad-ATF4DN or Ad-GFP for 24 h and exposed to HG for 72 h. JNK activation was evaluated by Western blot analysis. Results represent three independent experiments.
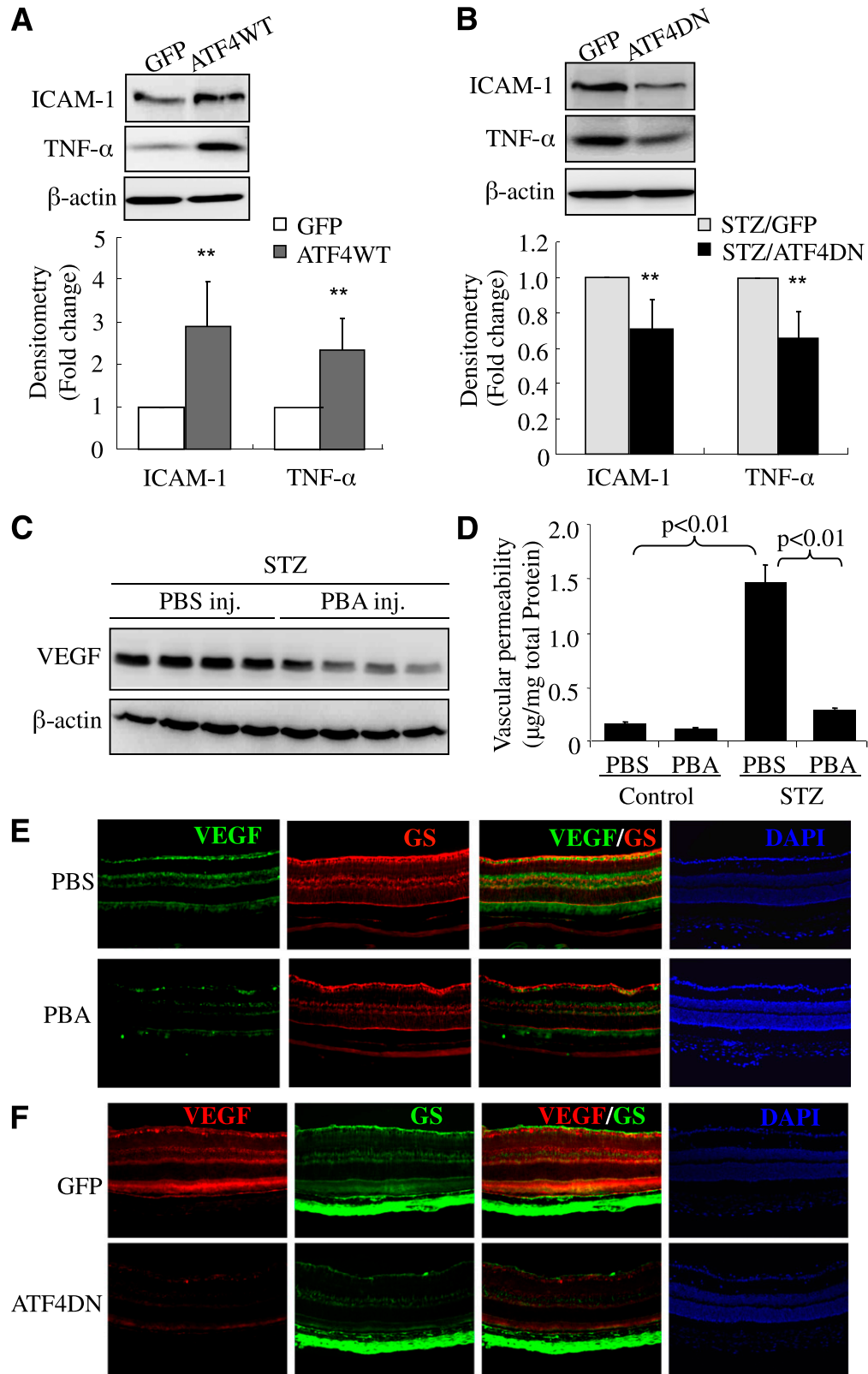
FIG. 7. Inhibition of ATF4 or suppression of ER stress ameliorates inflammatory gene expression and reduces vascular leakage in STZ-induced diabetic mice. *A*: Adult C57BL/6 J mice were given intravitreal injection of Ad-GFP or Ad-ATFWT (1×10^9 viral particles per eye). Two weeks after adenoviral injection, retinas were dissected and expression of proinflammatory factors (TNF-α and ICAM-1) was determined by Western blot analysis and quantified by densitometry (mean $\pm$ SD, $n = 8$). **$P < 0.01$. *B*: Four-week-old diabetic mice were randomly selected to receive an intravitreal injection of Ad-GFP or Ad-ATF4DN (1×10^9 viral particles per eye). Two weeks after injection, retinal levels of VEGF and ICAM-1 were evaluated by Western blot analysis (mean $\pm$ SD, $n = 3$). *C* and *D*: After onset of diabetes, STZ-induced diabetic mice received periocular injections of PBA (0.4 μmol/eye) into one eye and the same amount of vehicle into the contralateral eye twice a week for 6 weeks. Expression of VEGF in the retina (*C*) was measured by Western blot analysis and quantified by densitometry (mean $\pm$ SD, $n = 4$). Retinal vascular permeability (*D*) was measured by Evans blue albumin method. Results were expressed as microgram per milligram total retinal protein (mean $\pm$ SD, $n = 6$). Immunostaining of VEGF and GS in retinal sections from diabetic mice after PBA treatment (*E*) or Ad-ATF4DN treatment (*F*) as described above. Images represent four animals in each group. PBS, phosphate-buffered saline. (A high-quality digital representation of this figure is available in the online issue.)

High Glucose/Hypoxia

→

ER Stress ⊣ PBA
TUDCA

ATF4DN
ATF4 KO ⊣ ATF4 → HIF1α

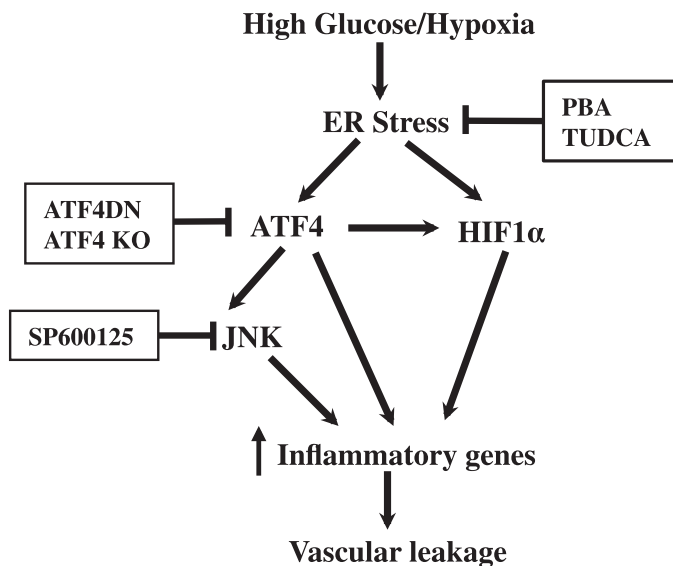SP600125 ⊣ JNK

↑ Inflammatory genes

→

Vascular leakage

FIG. 8. Schematic diagram showing the mechanisms of ER stress regulating inflammatory gene expression in retinal Müller cells. Diabetic insults such as hyperglycemia and hypoxia induce ER stress in retinal cells, including Müller cells. Unrelieved ER stress upregulates ATF4, which directly binds to promoters of inflammatory genes (e.g., VEGF), interacts and stabilizes HIF-1α, and activates JNK, resulting in exaggerated and sustained expression of inflammatory genes. Increased inflammatory cytokines promote leukostasis and endothelial activation, leading to breakdown of the blood-retinal barrier, vascular leakage, and diabetic macular edema.

reported that ER stress is enhanced in the retina in Akita mice, a genetic model of type 1 diabetes (11). Increased ER stress has also been reported in the kidney of diabetic rats and contributes to inflammation and apoptosis (25). However, how ER stress promotes inflammatory response and tissue injury remains poorly understood. In the current study, we demonstrated that ER stress–induced ATF4 plays an important role in this process. We found that two UPR branches mediated by IRE1-α and eIF2-α were activated at the early stage of DR. When compared with IRE1-α, diabetes induced a more intensive increase in eIF2-α phosphorylation in the retina, coincident with its downstream effectors ATF4 and CHOP. Moreover, intensive signal of ATF4 localized to the GCL and inner nuclear layer of the retina from diabetic mice (Fig. 1A). Although our data suggest that ATF4 contributes to Müller cell–derived inflammatory cytokine production, the role of ATF4 in retinal ganglion cells (RGCs) remains largely unknown. While loss of RGCs leading to neurodegeneration has been well studied in DR (26), significantly increased expression of inflammatory genes such as VEGF was observed in the retinal GCL in diabetic animals (Fig. 1B). Thus, we speculate that increased ATF4 expression may be associated with VEGF production from RGCs as well as with RGC death in diabetes. Indeed, recent studies demonstrate that ER stress is a key factor inducing RGC apoptosis in various conditions (27,28). The role of ATF4 in RGC-derived inflammatory cytokine production and RGC death in DR remains to be investigated.

Although diabetes initiates stress response in multiple cell types of the retina, data from our immunohistochemical study indicate that ER stress–triggered ATF4 activation and VEGF expression in Müller cells plays an important role in vascular leakage in the diabetic retina. In addition to Müller cells, other cell types in the retina also express VEGF, including astrocytes, RGCs, endothelial cells, and retinal pigment epithelial (RPE) cells (29). In the current study, double staining of VEGF and GS in retinal sections from diabetic mice shows that VEGF expression was partially expressed in Müller cells and colocalized with ATF4. Inhibition of ER stress or ATF4 markedly attenuated VEGF expression in the diabetic retina, accompanied by a decrease in other inflammatory gene expression (ICAM-1 and TNF-α) and reduction of vascular leakage. A recent study by Wang et al. (7) shows that conditional knockout of VEGF in retinal Müller cells significantly reduces leukostasis and vascular leakage in the diabetic retina, suggesting a critical role of Müller cell–derived VEGF in DR. However, the role of VEGF produced from other cell types, such as RGCs, in diabetes-induced vascular leakage should also be considered.

Our results indicate that ATF4 is essential for HG- and hypoxia-induced VEGF expression in retinal Müller cells. Previous studies show that ATF4 is required for the upregulation of VEGF by various stimuli, including homocysteine, arsenite, oxidized lipid, and growth factors in vascular cells and in RPE cells (30–32). In RPE cells, ATF4 binds to an amino-acid response element in the first intron of the VEGF gene (31). Indeed, we found that overexpression of ATF4 was sufficient to induce VEGF expression in retinal Müller cells and, conversely, inhibition of ATF4 significantly attenuated HG- and hypoxia-induced VEGF expression. In addition, inhibiting ER stress attenuated hypoxia-induced HIF-1α accumulation in Müller cells. Moreover, induction of ER stress by TM resulted in an increase in HIF-1α level, which was abrogated by inhibition of ATF4. Inhibition of ATF4 also abolished hypoxia-induced HIF-1α stabilization and nuclear translocation, suggesting that ATF4 is required for ER stress– and hypoxia-induced HIF-1α activation. However, neither overexpression of ATF4 nor inhibition of ATF4 activity alters the basal level of HIF-1α in Müller cells, suggesting that ATF4 alone is not sufficient to induce HIF-1α in normoxia. Future studies are needed to elucidate how ATF4 is involved in regulation of HIF-1α in a hypoxic condition and during ER stress.

In addition to HIF-1α, we found activation of JNK by ATF4 contributes to ER stress– and HG-mediated VEGF upregulation in retinal Müller cells. JNK is a stress-activated protein kinase and belongs to the superfamily of mitogen-activated protein kinases. Activation of JNK has been implicated in cell proliferation, apoptosis, and cytokine production (33). Recent studies show that JNK1 is critical for hypoxia-induced retinal VEGF production and neovascularization (19). Mice lacking JNK1 exhibit reduced pathological angiogenesis and lower levels of retinal VEGF production in oxygen-induced retinopathy (19). JNK1-mediated upregulation of VEGF is independent of HIF-1α activation, but through enhancing the binding of phospho–c-Jun to the VEGF promoter. In the current study, we found that HG treatment for 72 h induced activation of JNK1 in retinal Müller cells, which was abolished by chemical chaperones. Induction of ER stress resulted in enhanced JNK1 activation, while inhibition of JNK by specific JNK inhibitor completely prevented ER stress–induced VEGF upregulation. Moreover, overexpressing ATF4 was also sufficient to induce JNK activation, which was required for ATF4-mediated VEGF expression. These results suggest that ATF4 closely interacts with other proinflammatory pathways and, thus, may be a central coordinator for inflammatory response in Müller cells.

Although our results clearly indicate a role of ATF4 in regulation of ER stress–mediated inflammatory pathways in retinal cells, we do not exclude the role of other UPR

molecules, such as IRE1-α. We previously showed that activation of IRE1-α by TNF-α is implicated in upregulation of adhesion molecules in retinal endothelial cells through activation of the nuclear factor-κB (NF-κB) pathway (14). Activation of IRE1-α may also induce JNK activation, which upregulates inflammatory cytokines via transcription factor activating protein 1 and promotes cell apoptosis (34,35). In the current study, we found that ER stress and ATF4 upregulate ICAM-1 expression in retinal Müller cells. However, inhibition of JNK activation has no effect on ER stress– or ATF4-induced ICAM-1 expression, suggesting that JNK activation is not involved in regulation of ICAM-1 in Müller cells. In contrast, inhibitor of IκB kinase (IKK), an upstream activator of NF-κB, shows a significant inhibition of ICAM-1 expression in Müller cells exposed to HG, indicating that the NF-κB pathway is critical for HG-induced ICAM-1 upregulation (6). In mouse fibroblasts, ATF4 and NF-κB interact, occupy the promoter of platelet-derived growth factor receptor, and induce platelet-derived growth factor receptor transcription in a cooperative manner (36). Whether ATF4 affects NF-κB transcriptional activity and enhances ICAM-1 expression in retinal Müller cells remains to be investigated.

An interesting, and perhaps of clinical significance, finding in this study is the potent effects of PBA on inhibiting retinal VEGF expression and vascular leakage in diabetic animals. PBA is a small molecule chemical chaperone that stabilizes protein conformation, improves ER folding capacity, and facilitates the trafficking of mutant proteins (9). In 2006, Ozcan et al. (9) reported that treatment of obese and diabetic mice with PBA normalized blood glucose, restored insulin sensitivity, and enhanced insulin action in liver and peripheral tissues. We demonstrated that PBA inhibited hypoxia-induced VEGF expression in retinal endothelial cells and in mice with oxygen-induced retinopathy (11). Moreover, periocular injection of PBA significantly reduced retinal VEGF expression in Akita mice, suggesting that PBA regulates retinal VEGF expression independently of its effects on blood glucose (11). Consistently, in the current study we showed that local administration of PBA successfully prevented diabetes-induced retinal vascular leakage in STZ-induced diabetic mice. These results suggest that local delivery of PBA may hold promise as a potential therapeutic for retinal diseases that cause inflammation, vascular leakage, and macular edema, such as DR and age-related macular degeneration. It is notable that PBA has been used many years for the treatment of patients with urea cycle disorders, sickle-cell disease, thalassemia, and cystic fibrosis (37). Its potential effects on diabetes and diabetes complications warrant future investigation.

REFERENCES

1. Joussen AM, Poulaki V, Le ML, et al. A central role for inflammation in the pathogenesis of diabetic retinopathy. FASEB J 2004;18:1450–1452
2. Kern TS. Contributions of inflammatory processes to the development of the early stages of diabetic retinopathy. Exp Diabetes Res 2007;2007:95103
3. Li J, Wang JJ, Chen D, et al. Systemic administration of HMG-CoA reductase inhibitor protects the blood-retinal barrier and ameliorates retinal inflammation in type 2 diabetes. Exp Eye Res 2009;89:71–78
4. Zhang SX, Wang JJ, Gao G, Shao C, Mott R, Ma JX. Pigment epithelium-derived factor (PEDF) is an endogenous antiinflammatory factor. FASEB J 2006;20:323–325
5. Mizutani M, Gerhardinger C, Lorenzi M. Müller cell changes in human diabetic retinopathy. Diabetes 1998;47:445–449
6. Shelton MD, Distler AM, Kern TS, Mieyal JJ. Glutaredoxin regulates autocrine and paracrine proinflammatory responses in retinal glial (Müller) cells. J Biol Chem 2009;284:4760–4766
7. Wang J, Xu X, Elliott MH, Zhu M, Le YZ. Müller cell-derived VEGF is essential for diabetes-induced retinal inflammation and vascular leakage. Diabetes 2010;59:2297–2305
8. Yoshida H. ER stress and diseases. FEBS J 2007;274:630–658
9. Ozcan U, Yilmaz E, Ozcan L, et al. Chemical chaperones reduce ER stress and restore glucose homeostasis in a mouse model of type 2 diabetes. Science 2006;313:1137–1140
10. Kaser A, Lee AH, Franke A, et al. XBP1 links ER stress to intestinal inflammation and confers genetic risk for human inflammatory bowel disease. Cell 2008;134:743–756
11. Li J, Wang JJ, Yu Q, Wang M, Zhang SX. Endoplasmic reticulum stress is implicated in retinal inflammation and diabetic retinopathy. FEBS Lett 2009;583:1521–1527
12. Li J, Wang JJ, Yu Q, Chen K, Mahadev K, Zhang SX. Inhibition of reactive oxygen species by Lovastatin downregulates vascular endothelial growth factor expression and ameliorates blood-retinal barrier breakdown in db/db mice: role of NADPH oxidase 4. Diabetes 2010;59:1528–1538
13. Lange PS, Chavez JC, Pinto JT, et al. ATF4 is an oxidative stress-inducible, prodeath transcription factor in neurons in vitro and in vivo. J Exp Med 2008;205:1227–1242
14. Li J, Wang JJ, Zhang SX. Preconditioning with endoplasmic reticulum stress mitigates retinal endothelial inflammation via activation of X-box binding protein 1. J Biol Chem 2011;286:4912–4921
15. Malabanan KP, Khachigian LM. Activation transcription factor-4 and the acute vascular response to injury. J Mol Med (Berl) 2010;88:545–552
16. Gargalovic PS, Gharavi NM, Clark MJ, et al. The unfolded protein response is an important regulator of inflammatory genes in endothelial cells. Arterioscler Thromb Vasc Biol 2006;26:2490–2496
17. Poulaki V, Qin W, Joussen AM, et al. Acute intensive insulin therapy exacerbates diabetic blood-retinal barrier breakdown via hypoxia-inducible factor-1alpha and VEGF. J Clin Invest 2002;109:805–815
18. Kim H-T, Qiang W, Liu N, Scofield VL, Wong PK, Stoica G. Up-regulation of astrocyte cyclooxygenase-2, CCAAT/enhancer-binding protein-homology protein, glucose-related protein 78, eukaryotic initiation factor 2 alpha, and c-Jun N-terminal kinase by a neurovirulent murine retrovirus. J Neurovirol 2005;11:166–179
19. Guma M, Rius J, Duong-Polk KX, Haddad GG, Lindsey JD, Karin M. Genetic and pharmacological inhibition of JNK ameliorates hypoxia-induced retinopathy through interference with VEGF expression. Proc Natl Acad Sci U S A 2009;106:8760–8765
20. Zhang SX, Sima J, Shao C, et al. Plasminogen kringle 5 reduces vascular leakage in the retina in rat models of oxygen-induced retinopathy and diabetes. Diabetologia 2004;47:124–131
21. Zhang SX, Sima J, Wang JJ, Shao C, Fant J, Ma JX. Systemic and periocular deliveries of plasminogen kringle 5 reduce vascular leakage in rat models of oxygen-induced retinopathy and diabetes. Curr Eye Res 2005;30:681–689

22. Deng J, Lu PD, Zhang Y, et al. Translational repression mediates activation of nuclear factor kappa B by phosphorylated translation initiation factor 2. Mol Cell Biol 2004;24:10161–10168

23. Urano F, Wang X, Bertolotti A, et al. Coupling of stress in the ER to activation of JNK protein kinases by transmembrane protein kinase IRE1. Science 2000;287:664–666

24. Zhang K, Kaufman RJ. From endoplasmic-reticulum stress to the inflammatory response. Nature 2008;454:455–462

25. Liu G, Sun Y, Li Z, et al. Apoptosis induced by endoplasmic reticulum stress involved in diabetic kidney disease. Biochem Biophys Res Commun 2008;370:651–656

26. Kern TS, Barber AJ. Retinal ganglion cells in diabetes. J Physiol 2008;586:4401–4408

27. Shimazawa M, Inokuchi Y, Ito Y, et al. Involvement of ER stress in retinal cell death. Mol Vis 2007;13:578–587

28. Jing G, Wang JJ, Zhang SX. ER stress and apoptosis: a new mechanism for retinal cell death. Exp Diabetes Res 2012;2012:589589

29. Amin RH, Frank RN, Kennedy A, Eliott D, Puklin JE, Abrams GW. Vascular endothelial growth factor is present in glial cells of the retina and optic nerve of human subjects with nonproliferative diabetic retinopathy. Invest Ophthalmol Vis Sci 1997;38:36–47

30. Roybal CN, Yang S, Sun CW, et al. Homocysteine increases the expression of vascular endothelial growth factor by a mechanism involving endoplasmic reticulum stress and transcription factor ATF4. J Biol Chem 2004;279:14844–14852

31. Roybal CN, Hunsaker LA, Barbash O, Vander Jagt DL, Abcouwer SF. The oxidative stressor arsenite activates vascular endothelial growth factor mRNA transcription by an ATF4-dependent mechanism. J Biol Chem 2005;280:20331–20339

32. Malabanan KP, Kanellakis P, Bobik A, Khachigian LM. Activation transcription factor-4 induced by fibroblast growth factor-2 regulates vascular endothelial growth factor-A transcription in vascular smooth muscle cells and mediates intimal thickening in rat arteries following balloon injury. Circ Res 2008;103:378–387

33. Karin M, Gallagher E. From JNK to pay dirt: Jun kinases, their biochemistry, physiology and clinical importance. IUBMB Life 2005;57:283–295

34. Srivastava RK, Sollott SJ, Khan L, Hansford R, Lakatta EG, Longo DL. Bcl-2 and Bcl-X(L) block thapsigargin-induced nitric oxide generation, c-Jun NH (2)-terminal kinase activity, and apoptosis. Mol Cell Biol 1999;19:5659–5674

35. Vallerie SN, Furuhashi M, Fucho R, Hotamisligil GS. A predominant role for parenchymal c-Jun amino terminal kinase (JNK) in the regulation of systemic insulin sensitivity. PLoS ONE 2008;3:e3151

36. Zhang N, Khachigian LM. Injury-induced platelet-derived growth factor receptor-alpha expression mediated by interleukin-1beta (IL-1beta) release and cooperative transactivation by NF-kappaB and ATF-4: IL-1beta facilitates HDAC-1/2 dissociation from promoter [retracted in: J Biol Chem 2010;285:21902]. J Biol Chem 2009;284:27933–27943

37. Berg S, Serabe B, Aleksic A, et al. Pharmacokinetics and cerebrospinal fluid penetration of phenylacetate and phenylbutyrate in the nonhuman primate. Cancer Chemother Pharmacol 2001;47:385–390